

## Preparation of Discontinuous Alumina Fiber-Reinforced Iron-Matrix Composite by Spark Plasma Sintering

Hidekazu Sueyoshi<sup>1)</sup>, Tomohito Maruno<sup>2)</sup>, Yasushi Maeda<sup>2)</sup>  
and Tatsuro Onomoto<sup>3)</sup>

1) Department of Nano Structure and Advanced Materials, Graduate School of Science and Engineering,  
Kagoshima University, Kagoshima, 890-0065, Japan

Fax: 81-99-285-7704, e-mail: sueyoshi@mech.kagoshima-u.ac.jp

2) Graduate Student, Kagoshima University

3) Fukuoka Industrial Technology Center, Kitakyushu, Fukuoka, 807-0831, Japan

In order to obtain fundamental knowledge for processing of a discontinuous fiber-reinforced iron-matrix composite, spark plasma sintering of a mixture of discontinuous alumina fiber and pure iron powder was conducted. Alumina fiber is unreactive chemically to iron powder during SPS at 1173 K for 720 s. As the volume fraction of alumina fibers becomes large, the formation of micro-pore at alumina fiber/iron matrix interfaces and the formation of large pore at the alumina fiber-aggregated region occur, resulting in the increase in porosity. Therefore, the rate of hardening tends to decrease with increasing volume fraction of alumina fibers. Thus, the hardness disobeys a rule of mixtures. For alumina fiber-uniformly dispersed composite without fiber-aggregation, the critical volume fraction of alumina fibers exists, and it depends on the ratio of the particle diameter of iron powder to the diameter of alumina fiber. Based on this relationship, it is possible to obtain alumina fiber-uniformly dispersed composite.

Keywords: spark plasma sintering, discontinuous alumina fiber-reinforced iron-matrix composite, hardness, fiber uniform dispersion, a rule of mixtures

### 1. INTRODUCTION

When a fusion-solidification method is used as a production method of a fiber-reinforced iron-matrix composite, mechanical properties of fiber deteriorate because of overheating and reaction at fiber/liquid iron interfaces. Powder metallurgy that the preparation becomes feasible at low temperature compared with a fusion-solidification method is suitable for the preparation of fiber-reinforced iron-matrix composite.

We have examined the processing of continuous ceramic fiber/iron alloy composite by hot isostatic pressing and hot pressing, and have reported that the preparation of continuous ceramic fiber/iron alloy composite with uniform dispersion of fiber becomes feasible by choosing an appropriate combination of mixing method of fiber and iron alloy powder and sintering [1,2]. Also, we have examined spark plasma sintering (SPS) behavior of pure iron powder. The results revealed that decomposition of iron oxide film occurs during SPS, resulting in refining the surface of the iron powder [3]. Therefore, even SPS which was practiced at a relatively low temperature (1173 K) for a short holding time (720 s) enabled high densification [3]. Regarding the application of SPS to iron alloys, the results of high-Cr iron alloys [4-9], high-Cr cast iron [10-12], and Fe-0.8mass%C alloy [13] have been reported. However, there have been few reports of the application of SPS to fiber-reinforced iron-matrix composite. Also, there are a number of unclarified points regarding SPS behavior of a mixture of ceramic fiber and iron powder.

In the present study, in order to obtain fundamental knowledge for processing of a discontinuous

fiber-reinforced iron-matrix composite, discontinuous alumina fiber/iron composite was prepared by using SPS, the reaction between alumina fiber and iron powder, the influence of alumina fiber on the densification, applicability of a rule of mixtures, and a controlling factor in uniform dispersion of alumina fibers were examined in detail.

### 2. EXPERIMENTAL PROCEDURE

High-purity carbonyl iron powder (Mitsuiwa Chemical Co., Ltd.: Fe; 99.80 mass%, C; 0.01 mass%, N; <0.01 mass%, O; 0.15 mass%) having a mean particle diameter of 3.3  $\mu\text{m}$  was used [3]. The iron powder was a nearly spherical shape. As a discontinuous ceramic fiber,  $\alpha$ -alumina fiber (Denki Kagaku Kogyo Co., Ltd.:  $\text{Al}_2\text{O}_3$ ; 96.3 mass%,  $\text{SiO}_2$ ; 3.5 mass%,  $\text{Fe}_2\text{O}_3$ ; 0.2 mass%) having a density of 3.6  $\text{g/cm}^3$ , tensile strength of 700 MPa, elastic modulus of 93 GPa and Vickers hardness of  $H_V 800$  was used. Figure 1 shows a secondary electron (SE) image of alumina fibers. The alumina fibers had slightly different length, diameter and aspect ratio. Average diameter of alumina fibers was 3.0  $\mu\text{m}$ .

A mixture of alumina fiber and iron powder was packed into a graphite mold (inner diameter: 30 mm), followed by SPS (Sumitomo Coal Mining Co., Ltd.: PAS-III) in a vacuum (9.98 Pa). Figure 2 shows a schematic diagram of SPS process. At first, compaction was conducted under a pressure of 70 MPa. Thereafter pulsating current was passed for 60 s, followed by heating up to 1173 K and then holding with a pulse-less current. After holding for 720 s, the current was cut off

and then the sintered compact was slowly cooled. As mentioned above, a high-densification iron compact could be achieved under the same SPS condition [3].

We obtained a porosity of the alumina fiber/iron composite from the following equation:

$$P = (1 - V_0/V_s) \times 100 \quad \% \quad (1)$$

where  $P$  is the porosity,  $V_0$  is the theoretical volume ( $P=0\%$ ) obtained by dividing each mass of iron powder and alumina fiber in a mixture of iron powder and alumina fiber by each density of iron and alumina fiber, and  $V_s$  is the measured volume of the alumina fiber/iron composite.

The reaction between alumina fiber and iron powder was examined using an electron probe micro-analyzer (EPMA). Microstructure of the cross section of the alumina fiber/iron composite was examined using a scanning electron microscopy, and uniform dispersion of alumina fiber and the influence of alumina fiber on the densification were estimated on the basis of the results. In order to confirm applicability of a rule of mixtures, Vickers hardness (Shimadzu Co. Ltd., HMV-1/2) of the cross section of the alumina fiber/iron composite was measured under a load of 0.97 N.

### 3. RESULTS AND DISCUSSION

Figure 3 shows results of the EPMA analyses of alumina in the alumina fiber/iron composite prepared by SPS at 1173 K for 720 s. In SE image (Fig. 3(a)), gray part is an iron matrix, and black part is an alumina fiber.

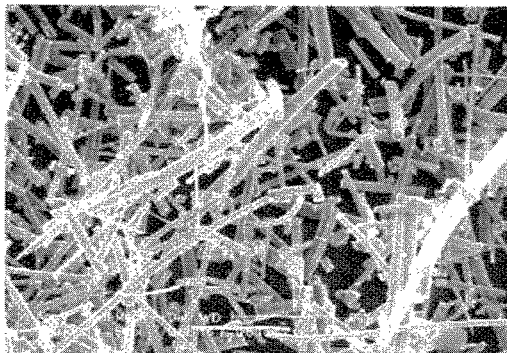


Fig. 1 SE image of alumina fibers.

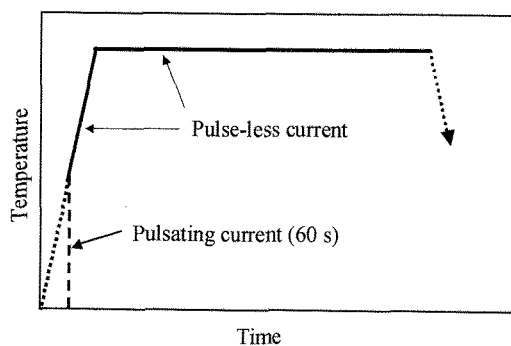
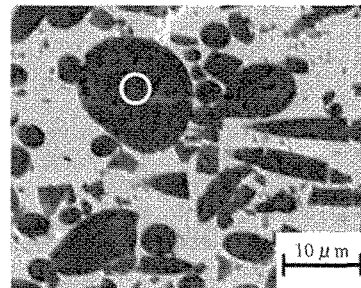


Fig. 2 Schematic diagram of SPS process.

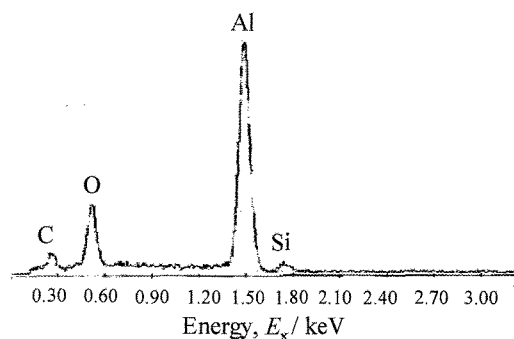
No damage of alumina fiber was observed. According to the result of qualitative analysis (the encircled area in Fig. 3(a)), the peak of C is due to a carbon deposition on the surface of the specimen. The peaks of Al, Si and O were confirmed in the alumina fiber as shown in Fig. 3(b). This result is similar to that of as-received alumina fiber. These results suggest that alumina fiber is unreactive chemically to iron powder during SPS.

Figure 4 shows SE images of the center of the cross section in the alumina fiber/iron composites. When the volume fraction of alumina fibers was 20 and 30 vol%, uniform dispersion of alumina fibers could be achieved. Also no large-pore was observed in the iron-matrix and at alumina fiber/iron matrix interfaces. In the alumina fiber/iron composite in which the volume fraction of alumina fibers was 40 vol%, not only a fiber-aggregated region but also a fiber-free region (white part) which was formed by falling off of alumina fiber from a specimen during a polishing operation were observed. When the volume fraction of alumina fibers was 50 vol%, fiber-aggregated and fiber-free regions increased. A large pore was also observed. These results suggest that there is an optimum volume fraction of alumina fibers for the preparation of the alumina fiber-uniformly dispersed composite.

Figure 5 shows the changes in Vickers hardness of the center of the cross section and porosity in the alumina fiber/iron composite with the volume fraction of alumina fibers. The porosity increased with increasing volume fraction of alumina fibers. As mentioned above, the iron compact having a high-densification was obtained under the same SPS conditions [3]. In addition, when the volume



(a)



(b)

Fig. 3 EPMA analyses of alumina in the alumina fiber/iron composite: (a) SE image, and (b) EDX analysis.

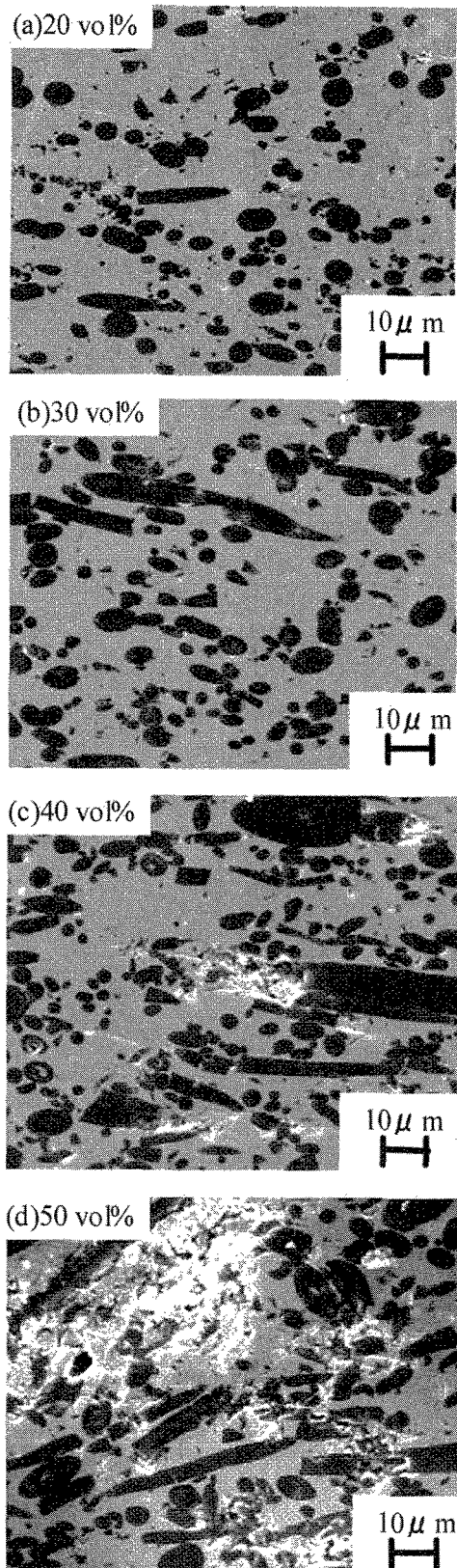


Fig. 4 SE images of the center of the cross section in the alumina fiber/iron composite

fraction of alumina fibers was 20 and 30 vol%, no large-pore was observed in the iron matrix and at alumina fiber/iron matrix interfaces (Figs. 4(a) and 4(b)). These results suggest that micro-pore was formed at alumina fiber/iron-matrix interfaces in the composite with small volume fraction of alumina fibers though it was unclear in Fig. 4(a) and 4(b). However, the porosity became large when the volume fraction of alumina fibers was very large (Fig. 5). This is because a packing of the iron powders was insufficient at the alumina fiber-aggregated regions, resulting in not only the formation of micro-pore but also the formation of large pore.

A rule of mixtures is expressed as follows:

$$H_{VC} = H_{VF} V_F + H_{VM}(1 - V_F) \quad (2)$$

where  $H_{VC}$  is Vickers hardness of the alumina fiber/iron composite,  $H_{VF}$  is Vickers hardness of alumina fiber,  $V_F$  is the volume fraction of alumina fibers, and  $H_{VM}$  is Vickers hardness of the iron matrix. Substituting  $H_{VF} = 800$  and  $H_{VM} = 120$  [3] into eq.(2), we obtained dashed line in Fig. 5. The experimental results disobeyed a rule of mixtures (dashed line). The rate of hardening tended to decrease with increasing volume fraction of alumina fibers. This may be caused by both the formation of micro-pore at alumina fiber/iron matrix interfaces and the formation of large pore at the alumina fiber-aggregated region as mentioned above. It is found from Fig. 5 that the influence of large pore on Vickers hardness of alumina fiber/iron composite is considerably large compared to that of micro-pore.

As mentioned above, when the volume fraction of alumina fibers was large, packing of the iron powders was insufficient at the alumina fiber-aggregated regions, resulting in the formation of large pore.

We examined a controlling factor in uniform dispersion of alumina fiber. Figure 6 shows schematic views of the closest packing. Based on the geometry, the following equations hold:

$$(d_{Fe} + d_{Fi}) \sin \pi / n = d_{Fe} \quad (3)$$

where  $d_{Fe}$  is the particle diameter of iron powder,  $d_{Fi}$  is the diameter of alumina fiber, and  $n$  is the number of

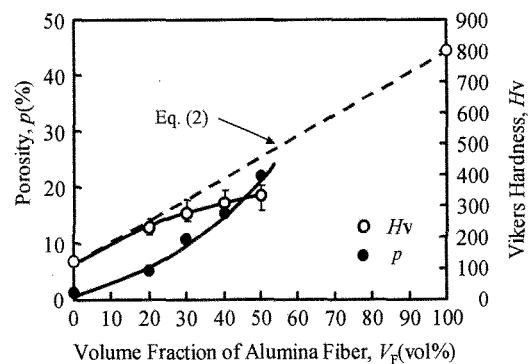


Fig. 5 Changes in Vickers hardness of the center of the cross section and porosity in the alumina fiber/iron composite with the volume fraction of alumina fibers.

iron powders surrounding alumina fiber. Let  $R=d_{Fe}/d_{Fi}$ , where  $R$  is the ratio of the particle diameter of iron powder to the diameter of alumina fiber. Substituting this relation into eq. (3) yields

$$\sin \pi / n = R / (R + 1) \quad (4)$$

Figure 7 shows the relationship between  $n$  and  $R$ . It is found that  $n$  decreases abruptly with increasing  $R$ . Substituting  $R=3.3/3.0=1.1$  (in this study) into eq. (4), we obtain  $n=6$  (Fig. 6(c)). Thus, the number of iron powders surrounding one alumina fiber depends on the ratio of the particle diameter of iron powder to the diameter of alumina fiber.

In sintering of a mixture of alumina fiber and iron powder, a part of the volume of iron powder surrounding alumina fiber is assigned to the nearest other alumina fiber. From Fig. 6, the number of iron powders,  $N_{CS}$ , which are substantially assigned to one alumina fiber with regard to a cross sectional direction of alumina fiber is given as follows:

$$N_{CS} = n/2 - 1 \quad (5)$$

Substituting  $n=6$  into eq. (5), we obtain  $N_{CS}=2$ . This means that the volume of two iron powders surrounds one alumina fiber with regard to a cross sectional direction of alumina fiber.

The number of iron powders which are arranged to one alumina fiber with regard to a longitudinal direction of alumina fiber,  $N_{LS}$ , is given by

$$N_{LS} = L_{Fi} / d_{Fe} \quad (6)$$

where  $L_{Fi}$  is the length of alumina fiber. The volume of one alumina fiber,  $V_{Fi}$ , is given as

$$V_{Fi} = \pi (d_{Fi} / 2)^2 L_{Fi} \quad (7)$$

From eqs. (5) and (6), the volume of iron matrix surrounding one alumina fiber,  $V_{Fe}$ , is

$$V_{Fe} = 4/3 \cdot \pi (d_{Fe} / 2)^3 N_{CS} N_{LS} \quad (8)$$

As a result, critical volume fraction of alumina fibers, at which alumina fiber-uniformly dispersed composite without fiber-aggregation is achieved, is expressed as

$$\begin{aligned} V_{CF} &= C V_{Fi} / (V_{Fi} + V_{Fe}) \times 100 \\ &= C / \{1 + 2/3 \cdot R^3 (n/2 - 1)\} \times 100 \quad \text{vol\%} \end{aligned} \quad (9)$$

where  $V_{CF}$  is critical volume fraction of alumina fibers, and  $C$  is the constant regarding dispersion morphology of alumina fiber. The value of  $C$  is 1 for a unidirectional arrangement, and that for a random arrangement is smaller than 1. Figure 8 shows the relationships between  $V_{CF}$  and  $R$  on the basis of eq. (9). It is found that  $V_{CF}$  decreases abruptly with increasing  $R$ . In Fig. 8, uniform dispersion without fiber-aggregation can be achieved below the curves. Experimental results were plotted in Fig. 8. The symbol  $\circ$  indicates uniform dispersion without fiber-aggregation, while the symbol  $\times$  indicates nonuniform dispersion with fiber-aggregation.

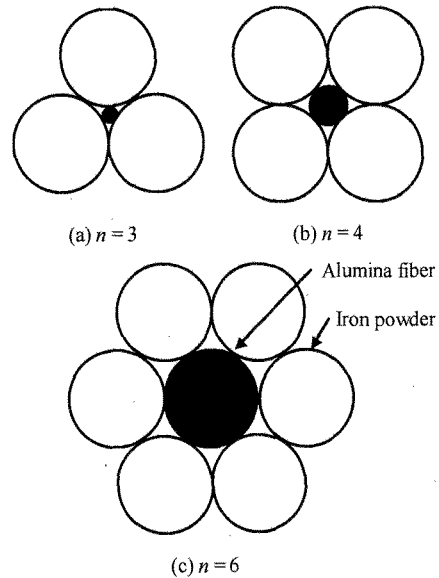


Fig. 6 Schematic views of the closest packing.

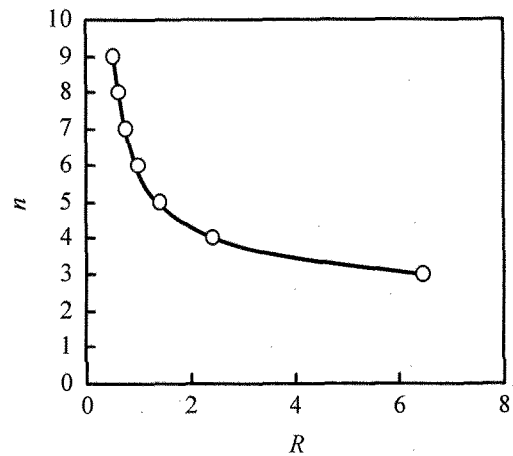


Fig. 7 Relationship between  $n$  and  $R$ .

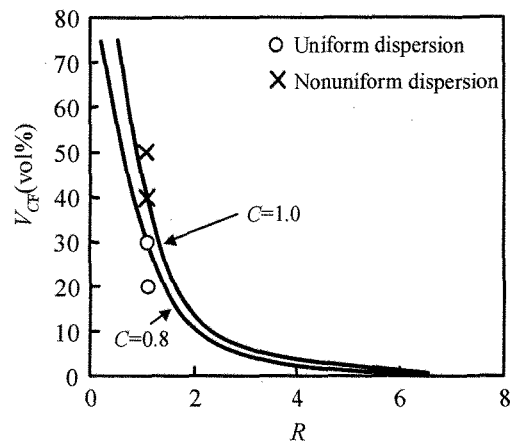


Fig. 8 Relationship between  $V_{CF}$  and  $R$  on the basis of eq. (9).

As shown in Fig. 8 experimental results agreed well with the curve of  $C=0.8$ . This is caused by a random arrangement of fibers. The above mentioned results suggest that eq. (9) holds. Based on eq. (9), it is possible to obtain alumina fiber-uniformly dispersed composite. eq. (9).

#### 4. CONCLUSIONS

In order to obtain fundamental knowledge for processing of a fiber-reinforced iron-matrix composite, SPS of a mixture of discontinuous alumina fiber and pure iron powder was conducted. From the results, the following conclusions were obtained.

(1) Alumina fiber is unreactive chemically to iron powder during SPS at 1173 K for 720 s.

(2) As the volume fraction of alumina fibers becomes large, not only the formation of micro-pore at alumina fiber/iron matrix interfaces but also the formation of large pore at the alumina fiber-aggregated region occur, resulting in the increase in porosity. Therefore, the rate of hardening tends to decrease with increasing volume fraction of alumina fibers. Thus the hardness disobeys a rule of mixtures.

(3) For alumina fiber-uniformly dispersed composite without fiber-aggregation, the critical volume fraction of alumina fibers exists, and it depends on the ratio of the particle diameter of iron powder to the diameter of alumina fiber. Based on this relationship, it is possible to obtain alumina fiber-uniformly dispersed composite.

#### REFERECES

1) H. Sueyoshi, T. Maruno, K. Yamamoto, Y. Hirata, S. Sameshima, S. Uchida, S. Hamauzu and S. Kurita, *Materials Trans.*, 43, 735-740 (2002).

2) H. Sueyoshi, T. Maruno, M. Asano, Y. Hirata, S. Sameshima, S. Uchida, S. Hamauzu and S. Kurita, *Materials Trans.*, 43, 2866-2872 (2002).

3) H. Sueyoshi, T. Maruno, Y. Maeda and T. Onomoto, Submitted to MRS-J.

4) N. Matsui, K. Kobayashi, A. Sugiyama and K. Ozaki, *J. Japan Society of Powder and Powder Metallurgy*, 44, 1121-1125 (1997).

5) N. Matsui, K. Kobayashi, A. Sugiyama and K. Ozaki, *J. Japan Society of Powder and Powder Metallurgy*, 45, 1081-1085 (1998).

6) N. Matsui, K. Matsui, K. Kobayashi, A. Sugiyama and K. Ozaki, *J. Japan Society of Powder and Powder Metallurgy*, 46, 1179-1184 (1999).

7) N. Matsui, K. Matsui, K. Kobayashi, A. Sugiyama and K. Ozaki, *J. Japan Society of Powder and Powder Metallurgy*, 47, 30-35 (2000).

8) N. Matsui, T. Yamada, K. Kobayashi, A. Sugiyama and K. Ozaki, *J. Japan Society of Powder and Powder Metallurgy*, 47, 332-336 (2000).

9) K. Kobayashi, A. Matsumoto, T. Nishio, K. Ozaki and A. Sugiyama, *J. Japan Society of Powder and Powder Metallurgy*, 47, 1097-1101 (2000).

10) T. Satoh, M. Sakamoto and H. N. Liu, *J. Japan Society of Powder and Powder Metallurgy*, 48, 1119-1125 (2001).

11) T. Satoh, H. N. Liu, M. Sakamoto, Y. Kawakami and K. Ogi, *J. Japan Society of Powder and Powder Metallurgy*, 50, 963-967 (2003).

12) T. Satoh, H. N. Liu, M. Sakamoto and Y. Kawakami, *J. Materials Science*, 40, 3283-3286 (2005).

13) H. W. Zhang, R. Gopalan, T. Mukai and K. Hono, *Scripta Materialia*, 53, 863-868 (2005).

(Received September 5, 2006; Accepted November 15, 2006)